Desalination and Water Treatment
www.deswater.com

doi: 10.5004/dwt.2021.26966

218 (2021) 294–302
April

A novel weighted mean-squared error optimization model to obtain optimal conditions of adsorption factors for a lead removal process

Akın Özdemir[a,*], Çağatay Teke[b], Hüseyin Serencam[c], Metin Uçurum[b], Ali Gündoğdu[d]

[a]*Industrial Engineering Department, Ondokuz Mayıs University, 55139 Samsun, Turkey, Tel. +90 3623121919/7610; email: akin.ozdemir@omu.edu.tr*
[b]*Industrial Engineering Department, Bayburt University, 69000 Bayburt, Turkey, Tel. +90 4582111153/1666; email: cagatayteke@bayburt.edu.tr (Ç. Teke), Tel. +90 4582111153/1676; email: mucurum@bayburt.edu.tr (M. Uçurum)*
[c]*Gastronomy and Culinary Arts, School of Applied Sciences, Trabzon University, 61300 Trabzon, Turkey, Tel. +90 4624551000; email: hserencam@trabzon.edu.tr*
[d]*Department of Pharmacy Services, Maçka Vocational School, Karadeniz Technical University, Maçka, 61750 Trabzon, Turkey, Tel. +90 4623777646; email: ramazan@ktu.edu.tr*

Received 15 July 2020; Accepted 31 December 2020

ABSTRACT

Lead (Pb) removal process from wastewater is an important issue to prevent health problems for people. For this particular purpose, a low-cost adsorbent may be beneficial for improving the adsorption capacity for the Pb removal process. The aims of this paper are four-fold. First of all, a *D*-optimal experimental design was selected to reduce experimental runs and its cost. Second, the effect of four adsorption design factors, stirring speed (rpm), adsorbent dosage (g), pH level, and initial metal concentration (ppm), was examined. Also, the yellow natural stone, which is from Bayburt, Turkey, was used as a cheap adsorbent for the Pb removal process from the solution. Third, a novel weighted mean-squared error optimization model was developed to obtain optimal adsorption levels for adsorption factors. Besides, a verification study was conducted to verify the results of the adsorption experiment. Finally, the lead (Pb(II)) removal capacity of the yellow Bayburt stone was obtained to be 46.031 mg/g, and the results of the experiment from the proposed methodology showed a good performance for the removal study.

Keywords: Adsorption; Lead; *D*-optimal experimental design; Optimization; Wastewater treatment

1. Introduction

Lead is toxic to people, plants, and animals, and it is known as a hazardous waste [1]. The presence of lead in water may cause some health problems leading to death for people. Therefore, it is crucial to enhance the adsorption capacity for a lead removal process to prevent health problems. In this paper, the effect of adsorption factors is investigated with a low-cost adsorbent for the Pb removal process from the solution.

A relevant literature review of lead removal studies was summarized as follows. First of all, Hamed et al. [2] studied electro-osmosis tests on saturated kaolinite specimens loaded using Pb(II) to examine the effectiveness and energy demand for the heavy metal removal process. Then, Bereket et al. [3] examined the adsorption process on

* Corresponding author.

bentonite for the removal process of Pb(II), Cd(II), Zn(II), and Cu(II) from aqueous solutions. Along the same lines, Reed et al. [4] investigated the removal process of As(III), As(V), Hg(II), and Pb(II) by virgin and Fe(III) impregnated activated carbons. Next, Naseem and Tahir [5] used bentonite as an adsorbent for the removal of Pb(II) from aqueous and acidic solutions. Further, Taty-Costodes et al. [6] conducted batch experiments to study the main factors for the removal of Cd(II) and Pb(II) ions. Besides, Wong et al. [7] studied tartaric acid modified rice husk from aqueous solutions for the Cu and Pb removal processes. Then, Bulut and Baysal [1] observed the removal process of Pb(II) ions from aqueous solutions with wheat bran. Besides, Amarasinghe and Williams [8] studied to compare commonly used absorbents and tea waste in the removal process of Cu and Pb from aqueous wastewater. Then, Xu et al. [9] used oxidized multiwalled carbon nanotubes as a sorbent to investigate the sorption characteristic for the Pb(II) removal from aqueous solution. Further, Yetilmezsoy et al. [10] used a Box–Behnken experimental design with response surface methodology and a quadratic programming method to maximize Pb(II) removal from aqueous solution by *Pistacia vera* L. Besides, Nassar [11] employed magnetic nano adsorbents for the Pb(II) removal while applying a batch-adsorption method. Next, Al-zboon et al. [12] studied to synthesize a highly amorphous geopolymer from waste cool fly ash by using an adsorbent for a Pb removal process from wastewater. Along the same lines, Zhao et al. [13] used the prepared few-layered graphene oxide to adsorb Pb(II) from aqueous solutions. Further, Madadrang et al. [14] investigated an adsorption behavior of ethylenediamine tricrotic acid-graphene oxide for the Pb(II) removal process. Next, Kim et al. [15] showed that a zeolite-nanoscale zero-valent iron composite is a good alternative for the Pb removal process from wastewater.

For recent lead removal studies in the literature, Liu et al. [16] evaluated the efficiencies of fly ash, fly ash-based geopolymer, and faujasite block as sorbents for the Pb removal process from aqueous solutions. Besides, Ma et al. [17] studied porous lignin-based poly/organo-montmorillonite nanocomposites with salt tolerance and as an adsorbent for the Pb(II) removal process from wastewater. Further, Liu et al. [18] synthesized activated carbon-supported nanoscale zero-valent iron composite at ultralow iron content for the Pb(II) removal process. Finally, Lin et al. [19] synthesized iron nanoparticles adsorbent in one-step with green tea extract for the removal of both Pb(II) and rifampicin at the same time from wastewater.

In the literature, Vining and Myers [20] proposed a dual response model to find an optimal solution for design factors. However, this model may result in an infeasible solution due to a strict target assumption. Therefore, Cho [21], and Lin and Tu [22] separately proposed a relaxed target assumption with the mean-squared error (MSE) optimization approach. These MSE models have equal priorities for process bias and variance. Besides, the process bias is the difference between the process mean and target. Next, Cho et al. [23], and Köksoy and Doganaksoy [24] separately proposed the weighted MSE (WMSE) models. It is also noted that Köksoy and Doganaksoy [24] used Pareto optimal solutions to generate alternative solutions. Along the same lines, Cho et al. [25] modified the MSE model while considering symmetric quality loss function. Besides, Ding et al. [26], and Shin et al. [27] proposed WMSE models with the weighted sum method in the multi-objective optimization concept. Then, Köksoy [28] and Park et al. [29] used forth-order parameters to optimize design factors with WMSE models. Further, Ozdemir and Cho [30] proposed a mixed-integer nonlinear programming model with a Box–Behnken design while considering the process bias and variance at the same time. Finally, Ozdemir and Cho [31] developed a 0–1 mixed-integer nonlinear programming model by using a factorial design with pseudo-center points to simultaneously optimize the process bias and variance for both qualitative and quantitative design factors.

The contributions of this paper are four-fold. One, a *D*-optimal experimental design was selected over other experimental designs to reduce experimental runs and their cost. In addition, an exchange algorithm was used to construct *D*-optimal experimental design points. Also, the generated *D*-optimal experimental design provided model parameter estimation. Two, the effect of four design factors, including stirring speed (rpm), adsorbent dosage (g), pH level, and initial metal concentration (ppm) on lead adsorption was investigated. Besides, the yellow Bayburt stone (YBS), which is a natural stone in Bayburt, Turkey, was used as an adsorbent for the lead removal from aqueous solutions. It is also noted that this study is the first research attempt to use the YBS as an efficient, inexpensive, and cheap adsorbent for the Pb(II) removal process. Three, a novel WMSE optimization model was proposed to obtain optimal adsorption levels for each adsorption factor. The results of the proposed optimization method showed good performance, and the optimization results are consistent with the experimental results. Finally, a verification study was conducted to validate the results of the experiment.

The rest of this paper was organized as follows. First of all, the proposed methodology development is presented in Section 2. Then, the materials used were provided in Section 3. Next, the results of the experiment were presented in Section 4. The results were discussed in Section 5. Finally, concluding remarks were drawn in Section 6.

2. Proposed methodology

The five-phased proposed methodology is presented as follows: (1) the planning phase, (2) the experimental phase, (3) the modeling phase, (4) the optimization phase, and (5) the verification phase.

2.1. Planning phase

In the planning phase, design factors are determined to conduct an adsorption experimental design. Besides, the coded and uncoded units define each factor levels in the adsorption experimental design. In this paper, an experimental design uses –1, 0, and +1 notation to denote the low level, the center level, and high level, respectively, for each design factor. The use of –1, 0, and +1 for the design factor setting is called the coded units. On the other hand, the actual values of each coded unit denote the uncoded units.

Indeed, the use of the coded units aids in the interpretation of the coefficients that fit a specified experimental model.

2.2. Experimental phase

An experimenter may want to reduce the number of experimental runs required by a traditional response surface experimental design. For example, a Box–Behnken experimental design requires 27 experimental runs to fit a second-order model in four design factors. On the other hand, the second-order model has 15 terms. In order to reduce the number of experimental runs, the *D*-optimal experimental design is selected over other response surface experimental designs. Besides, the *D*-optimal experimental design uses the *D*-optimality criterion and focuses on model parameter estimation [32].

The *D*-optimality criterion is to maximize the determinant of the moment matrix, M, and is defined as follows:

$$\text{maximize } \det\left[\mathrm{M}\right] \tag{1}$$

where M = |X′X|/*N*, X is a model matrix, X′ is a transpose of the model matrix, and *N* is the number of experimental runs. Besides, the *D*-efficiency is calculated as $|(\mathrm{X'X})^{-1}|^{1/\text{a number of parameters in the model}}/N$.

In the literature, Eq. (1) can be solved with an exchange algorithm to generate *D*-optimal experimental design points [32]. In this paper, the exchange algorithm is used to construct design points for the adsorption experiment. The running time (seconds) of the algorithm was calculated by the JMP software. The change (%) was calculated differences between the *D*-efficiencies while considering the consecutive runs.

2.3. Modeling phase

In this paper, a full second-order model is used, including first-order, interaction, and quadratic terms. The fitted second-order model for the process mean is as follows:

$$\hat{\mu}(\mathrm{x}) = \hat{\alpha}_0 + \mathrm{x}^T\mathrm{a} + \mathrm{x}^T\mathrm{A}\mathrm{x} \text{ where } \mathrm{x} = \begin{bmatrix} x_1 \\ x_2 \\ \cdots \\ \cdots \\ \cdots \\ x_k \end{bmatrix},\ \mathrm{a} = \begin{bmatrix} \hat{\alpha}_1 \\ \hat{\alpha}_2 \\ \cdots \\ \cdots \\ \cdots \\ \hat{\alpha}_k \end{bmatrix}, \text{ and } \mathrm{A} = \begin{pmatrix} \hat{\alpha}_{11}\ \ \hat{\alpha}_{12}/2 \ \ldots\ \hat{\alpha}_{1k}/2 \\ \cdots \\ \cdots \\ \cdots \\ \hat{\alpha}_{k1}/2\ \ \hat{\alpha}_{k2}/2 \ \ldots\ \hat{\alpha}_{kk} \end{pmatrix} \tag{2}$$

where $\hat{\mu}(\mathrm{x})$ is the fitted response function of the mean, and $\hat{\alpha}_i$ is the *i*th regression coefficient (*i* = 0, 1, 2, …, *k*). Besides, x is the vector of the design factors of the experiment. Also, vector a and matrix A represent the estimated regression coefficients of the process mean. At the same time, the fitted second-order model for the process standard deviation is denoted as follows:

$$\hat{\sigma}(\mathrm{x}) = \hat{\beta}_0 + \mathrm{x}^T\mathrm{b} + \mathrm{x}^T\mathrm{B}\mathrm{x} \text{ where } \mathrm{x} = \begin{bmatrix} x_1 \\ x_2 \\ \cdots \\ \cdots \\ \cdots \\ x_k \end{bmatrix},\ \mathrm{b} = \begin{bmatrix} \hat{\beta}_1 \\ \hat{\beta}_2 \\ \cdots \\ \cdots \\ \cdots \\ \hat{\beta}_k \end{bmatrix}, \text{ and } \mathrm{B} = \begin{pmatrix} \hat{\beta}_{11}\ \ \hat{\beta}_{12}/2 \ \ldots\ \hat{\beta}_{1k}/2 \\ \cdots \\ \cdots \\ \cdots \\ \hat{\beta}_{k1}/2\ \ \hat{\beta}_{k2}/2 \ \ldots\ \hat{\beta}_{kk} \end{pmatrix} \tag{3}$$

where $\hat{\sigma}(\mathrm{x})$ is the fitted response function of the standard deviation, and $\hat{\beta}_i$ is the *i*th regression coefficient (*i* = 0, 1, 2, …, *k*). Besides, vector b and matrix B represent the estimated regression coefficients of the process standard deviation. Similarly, the fitted second-order model for the process variance is as follows:

$$\hat{\sigma}^2(\mathrm{x}) = \hat{\delta}_0 + \mathrm{x}^T\mathrm{c} + \mathrm{x}^T\mathrm{C}\mathrm{x} \text{ where } \mathrm{x} = \begin{bmatrix} x_1 \\ x_2 \\ \cdots \\ \cdots \\ \cdots \\ x_k \end{bmatrix},\ \mathrm{c} = \begin{bmatrix} \hat{\delta}_1 \\ \hat{\delta}_2 \\ \cdots \\ \cdots \\ \cdots \\ \hat{\delta}_k \end{bmatrix}, \text{ and } \mathrm{C} = \begin{pmatrix} \hat{\delta}_{11}\ \ \hat{\delta}_{12}/2 \ \ldots\ \hat{\delta}_{1k}/2 \\ \cdots \\ \cdots \\ \cdots \\ \hat{\delta}_{k1}/2\ \ \hat{\delta}_{k2}/2 \ \ldots\ \hat{\delta}_{kk} \end{pmatrix} \tag{4}$$

where $\hat{\sigma}^2(\mathrm{x})$ is the fitted response function of the variance, and $\hat{\delta}_i$ is the *i*th regression coefficient (*i* = 0, 1, 2, …, *k*). Besides, vector c and matrix C represent the estimated regression coefficients of the process variance. Please notice that $\hat{\sigma}(\mathrm{x}) \neq \hat{\sigma}^2(\mathrm{x})$ because of the different regression coefficients.

2.4. Optimization phase

A novel WMSE model is proposed to obtain optimal conditions of adsorption factors for a lead removal process from the solution. The objective function of the proposed model is to minimize a WMSE function while assigning weights for each term in the function. The first term is related to the process bias, and the second term is related to the variability measure. Besides, the variability measure could be either the process standard deviation or the process variance. The selection of variability measures could affect an optimal solution of adsorption factors for the lead removal process. Besides, the variability measure with the highest R^2 (coefficient of determination) is selected for the optimization phase because the R^2 is a statistical measure of how well the second-order regression prediction approximates the adsorption data. The model is subject to constraints. The first constraint is related to weights and the sum of weights is one. Besides, the second constraint is related to the non-negative process standard deviation or variance. Other constraints are the boundary constraints for design factors. The proposed optimization model is denoted as follows:

$$\begin{aligned}
&\text{minimize } w_1\left[\hat{\mu}(\mathrm{x})-\mu_\tau\right]^2+w_2\left[\hat{\sigma}(\mathrm{x})\right]^2 \text{ or } w_1\left[\hat{\mu}(\mathrm{x})-\mu_\tau\right]^2\\
&\quad +w_2\left[\hat{\sigma}^2(\mathrm{x})\right]\\
&\text{subject to}\\
&w_1+w_2=1\\
&\hat{\sigma}(\mathrm{x})\geq 0 \text{ or } \hat{\sigma}^2(\mathrm{x})\geq 0\\
&\mathrm{LB}\leq x_i\leq \mathrm{UB}\ (i=1,\ 2,\ \ldots,\ k);\ \forall x_i\in R
\end{aligned} \tag{5}$$

where $\hat{\mu}(\mathrm{x})$ is the estimated process mean, μ_τ is the desired target value by the experiment, $\hat{\mu}(\mathrm{x})$ — μ_τ is the process bias, $\hat{\sigma}(\mathrm{x})$ is the estimated process standard deviation, $\hat{\sigma}^2(\mathrm{x})$ is the estimated process variance, x_i is the ith design factor, LB is the lower bound for design factors, and UB is the upper bound for design factors. Besides, w_1 and w_2 denote weights for each term in the objective function. It is also noted that MATLAB software with the fmincon command is used to solve the proposed optimization model in Eq. (5).

In this paper, the different number of cases is considered for the proposed optimization model while assigning different weights for each term. Therefore, many cases are analyzed to obtain optimal conditions of design factors. For example, minimizing the process bias may be more important than minimizing the process standard deviation. For these particular cases, the weight of the process bias is bigger than 0.5 to meet this specific process requirement. Thus, the decision-maker decides to assign weights for each term while considering the process requirements.

2.5. Verification phase

The verification phase consists of two parts. The first step is to compare the results from the proposed optimization model and the results of the traditional dual response optimization model. It is expected that the proposed optimization model may improve the optimal conditions of design factors from the traditional counterpart. The traditional optimization model is denoted as follows:

$$\begin{aligned}
&\text{minimize } \hat{\sigma}(\mathrm{x})\\
&\text{subject to } \hat{\mu}(\mathrm{x})=\mu_\tau\\
&\qquad\quad \mathrm{LB}\leq x_i\leq \mathrm{UB}\ (i=1,\ 2,\ \ldots,\ n);\ \forall x_i\in R
\end{aligned} \tag{6}$$

The second step is to run an adsorption experiment using optimal conditions to verify the optimum results from the proposed optimization model.

3. Materials

In this study, the yellow Bayburt stone (YBS), located in Bayburt, Turkey, was used. After each sample was broken under 2 mm in a jaw crusher, it was ground to 250 microns in a ball mill with a stainless steel body and used in experiment runs.

The chemical analysis of the YBS is given in Table 1. The YBS is a low amorphous stone and contains calcite, quartz, feldspar group minerals, clay group minerals, and pyroxene group minerals [33]. It is a scientific fact that these minerals are used as adsorbents. In this paper, the YBS, which contains all of these minerals, was used as an adsorbent.

The mass of metal ions adsorbed (MIA) is calculated as follows:

$$\mathrm{MIA}=\frac{\left(C_0-C\right)\times V}{m\times 1{,}000} \tag{7}$$

where the mass of MIA is metal ions/sample (mg/g). Also, C_0 and C are the concentration (ppm) of metal ions before and after the incubation period, respectively. Besides, V and m are the aqueous step volume (mL) and the adsorbent amount (g), respectively.

4. Results of the experiment

The four adsorption factors were specified as stirring speed (rpm), adsorbent dosage (g), pH level, and initial metal concentration (ppm). The four adsorption factors and their levels are given in Table 2. Besides, the contact time was specified as 30 min for the experiment.

Table 3 compares experimental designs based on the necessary number of runs for four adsorption factors. As shown in Table 3, the D-optimal experimental design provides the fewest design points for the adsorption experiment. Besides, the D-optimality criterion works well to minimize the generalized variance of the parameter estimates for a full second-order model. Therefore, the D-optimal experimental design was selected for the adsorption experiment. The D-optimal experimental design is cost-effective in terms of the number of experimental runs. Besides, the D-optimal experimental design provides time efficiency comparing other response surface designs in Table 3.

Table 1
Chemical analysis of the YBS [33]

Oxides	Percentage (%)
SiO_2	70.32
Al_2O_3	11.01
Fe_2O_3	0.83
CaO	2.87
MgO	0.87
SO_3	0.15
Na_2O	1.36
K_2O	1.79
Total alkali	2.54

Table 2
Four adsorption factors and their levels

Adsorption factor	Levels		
	–1 (Low)	0 (Center)	1 (High)
x_1: stirring speed (rpm)	500	750	1,000
x_2: adsorbent dosage (g)	0.50	0.75	1.00
x_3: pH level	2	4	6
x_4: initial metal concentration (ppm)	100	200	300

Table 3
Comparison of the designs for the experiment based on the necessary number of runs

Necessary number of runs	Experimental design
27	Box–Behnken design
26	Traditional central composite design (CCD)
30	CCD – orthogonal blocks
31	CCD – uniform precision
36	CCD – orthogonal
15 or more	*D*-optimal experimental design

Table 4
D-efficiency values for the specified runs

Run	*D*-efficiency (%)	Running time (s)	Change (%)
15	42.50	150.169	–
16	43.39	139.303	2.09
17	44.52	135.896	2.60
18	45.49	149.884	2.18
19	46.16	133.535	1.47
20	**46.56**	**138.080**	**0.87**
21	46.80	135.636	0.52
22	47.05	141.217	0.53
23	47.09	134.102	0.09
24	47.24	130.555	0.32
25	47.75	135.831	1.08

Table 4 shows the values of the *D*-efficiency (%), the running time (s), and the change (%) for each specified run. It was decided to run the 20-point *D*-optimal design due to the number of resources and time allowed for the adsorption experiment. As shown in Table 4, too many runs may slightly increase the *D*-efficiency value. Besides, the change is below 1.25% after the 20 runs. Therefore, the 20-point design points are sufficient to experiment.

In Table 5, the 20-point *D*-optimal design was replicated two times for the experiment. Besides, y_{u1} is the result of the *u*th experimental run for the first replicate, and y_{u2} is the result of the *u*th experimental run for the second replicate. Also, y_{u1} (mg/g) and y_{u2} (mg/g) were found using Eq. (7) for each run. Next, $\bar{y}_u$ is the dependent variable (response) for the experiment, and it is the average of y_{u1} and y_{u2} for each run. Besides, s_u and s_u^2 are the standard deviation and variance of y_{u1} and y_{u2}, respectively.

Figs. 1 and 2 show the prediction variance profile and the fraction of the design space plot, respectively. It is also noted that Figs. 1 and 2 are drawn using the JMP software. The prediction variance profile in Fig. 1 is helpful to figure out where in the experimental design space the predictions have more or less variability. Besides, a low prediction variance is desired. The value of the prediction variance is 0.791 when stirring speed = 750 rpm, the adsorbent dosage = 0.75 g, pH = 4, and initial metal concentration = 200 ppm. On the other hand, several factor settings may have the same relative variance. The fraction of the design space plot shows the proportion of the experimental design space over which the relative prediction variance lies below a specified value. Fig. 2 shows that the minimum relative prediction variance is less than 0.3, while the maximum is below 2.5. The red dotted crosshairs denote that the relative prediction variance is less than 0.62 over about 50% of the design space.

The fitted complete second-order models for the process mean, standard deviation, and variance is denoted using Eqs. (2)–(4) as follows:

$$\begin{aligned}\hat{\mu}(x) &= 26.815 + 0.070x_1 - 9.798x_2 + 0.327x_3 + 14.777x_4 - 0.383x_1^2 \\ &+ 2.763x_2^2 + 0.150x_3^2 + 0.179x_4^2 - 0.092x_1x_2 + 0.394x_1x_3 \\ &- 0.312x_1x_4 + 0.181x_2x_3 - 5.047x_2x_4 + 0.273x_3x_4 \\ (R^2 &= 99.94\%)\end{aligned} \tag{8}$$

$$\begin{aligned}\hat{\sigma}(x) &= 0.181 - 0.078x_1 - 0.075x_2 + 0.076x_3 + 0.037x_4 - 0.045x_1^2 \\ &- 0.005x_2^2 + 0.036x_3^2 - 0.033x_4^2 + 0.069x_1x_2 - 0.122x_1x_3 \\ &- 0.013x_1x_4 - 0.096x_2x_3 + 0.012x_2x_4 + 0.006x_3x_4 \\ (R^2 &= 83.49\%)\end{aligned} \tag{9}$$

$$\begin{aligned}\hat{\sigma}^2(x) &= 0.025 - 0.061x_1 - 0.057x_2 + 0.060x_3 + 0.021x_4 + 0.001x_1^2 \\ &+ 0.011x_2^2 + 0.026x_3^2 + 0.004x_4^2 + 0.069x_1x_2 - 0.081x_1x_3 \\ &- 0.013x_1x_4 - 0.078x_2x_3 - 0.003x_2x_4 + 0.009x_3x_4 \\ (R^2 &= 80.16\%)\end{aligned} \tag{10}$$

The estimated process standard deviation is selected as a variability measure for the optimization phase because the R^2 value of the estimated process standard deviation is higher than the R^2 value of the estimated process variance. MATLAB software with the fmincon command was used to obtain optimal conditions for the adsorption experiment. Besides, the initial points are specified as [–1 –1 –1 –1]. The results of the proposed WMSE optimization model in Eq. (11) are denoted in Table 6 with the estimated process standard deviation for the adsorption experiment. The desired target value is specified as 45 mg/g based on the process requirement specified by the experimenter. It is also noted that the different target values could affect the results of the proposed WMSE optimization model.

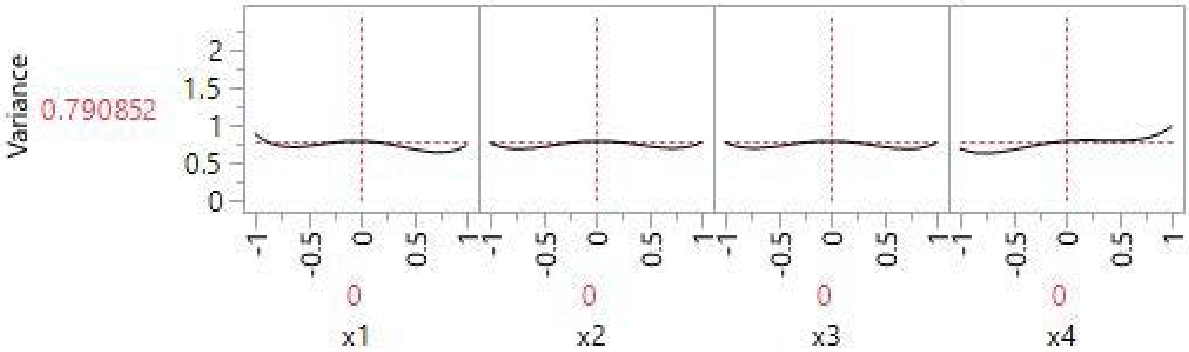

Fig. 1. Prediction variance profile.

In Table 6, the first case is not a desired solution for the adsorption experiment because the process bias is very high. The reason is that the model minimizes the estimated process standard deviation without considering the process bias when $w_1 = 0$. The proposed optimization model in Eq. (5) minimizes the process bias and standard deviation at the same time. In Table 6, the 11 different numbers of cases are considered for the proposed optimization model while assigning different weights for each term. Particularly, the fifth case provides the smallest process standard deviation while not to consider the first case. Besides, the process bias is very little for the fifth case. Also, the fifth case was assigned more weight for the process standard deviation. This assumption is consistent in the context of the quality engineering problems, and the process standard deviation reduction is an important issue to reduce the variability of the experiment.

$$
\begin{aligned}
\text{minimize } & w_1\begin{bmatrix} 26.815+0.070x_1-9.798x_2+0.327x_3+14.777x_4 \\ -0.383x_1^2+2.763x_2^2+0.150x_3^2+0.179x_4^2 \\ -0.092x_1x_2+0.394x_1x_3-0.312x_1x_4+0.181x_2x_3 \\ -5.047x_2x_4+0.273x_3x_4-45 \end{bmatrix}^2 \\
& + w_2\begin{bmatrix} 0.181-0.078x_1-0.075x_2+0.076x_3+0.037x_4 \\ -0.045x_1^2-0.005x_2^2+0.036x_3^2-0.033x_4^2 \\ +0.069x_1x_2-0.122x_1x_3-0.013x_1x_4-0.096x_2x_3 \\ +0.012x_2x_4+0.006x_3x_4 \end{bmatrix}^2 \\
\text{subject to} & \\
& w_1+w_2=1 \\
& 0.181-0.078x_1-0.075x_2+0.076x_3+0.037x_4-0.045x_1^2 \\
& -0.005x_2^2+0.036x_3^2-0.033x_4^2+0.069x_1x_2-0.122x_1x_3 \\
& -0.013x_1x_4-0.096x_2x_3+0.012x_2x_4+0.006x_3x_4 \geq 0 \\
& -1 \leq x_i \leq +1 \ (i=1,\ 2,\ 3,\ 4);\ \forall x_i \in R
\end{aligned}
\tag{11}
$$

For the comparison study, the optimum results of the proposed WMSE optimization model and the optimum results of the traditional dual response surface model proposed by Vining and Myers [20] are compared. The results of the Vining and Myers [20] model are $x_1 = 1.0000$, $x_2 = -0.1783$, $x_3 = 0.9968$, and $x_4 = 0.9997$. Besides, the estimated standard deviation of the Vining and Myers [20] model is 0.0664, and the process bias is 0. The results of the Vining and Myers [20] model are similar to the 11th case of the proposed model. However, the fifth case of the proposed model is superior to the Vining and Myers [20] model because the fifth case can reduce more the estimated standard deviation value than the Vining and Myers [20] model.

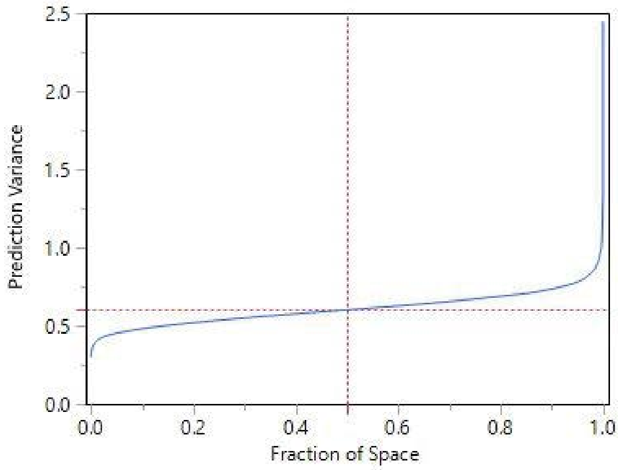

Fig. 2. Fraction of the design space plot.

For the verification study, an experiment was conducted using the optimal results of the fifth case of the proposed optimization model. The results of coded adsorption factors are $x_1 = 1.0000$, $x_2 = -0.2294$, $x_3 = 0.3381$, and $x_4 = 0.9964$. For uncoded levels, stirring speed is 1,000 rpm, the adsorbent dosage is 0.69 g, pH is 4.7, and the initial metal concentration is 299.64 ppm. The mean value of the actual experiment is 46.031 mg/g. Both the optimization and actual results are consistent in terms of the process mean.

Some studies on natural inorganic adsorbents are presented in Table 7. The YBS shows good performance as a low-cost adsorbent based on the comparison studies.

5. Discussions

Each design factor was analyzed and the following observations were made. First of all, the stirring speed

Table 5
20-point *D*-optimal design replicated two times and collected data

Run	Adsorption factors				Collected data				
	x_1	x_2	x_3	x_4	y_{u1}	y_{u2}	$\bar{y}_u$	s_u	s_u^2
1	1.00	–1.00	1.00	1.00	59.908	59.938	59.923	0.021	0.0004
2	–1.00	1.00	1.00	–1.00	9.977	9.947	9.962	0.021	0.0004
3	–1.00	1.00	–1.00	–1.00	9.706	9.647	9.677	0.042	0.0018
4	–1.00	–1.00	–1.00	–1.00	19.362	19.328	19.345	0.024	0.0006
5	1.00	1.00	–1.00	–1.00	9.679	9.639	9.659	0.028	0.0008
6	–1.00	–1.00	–1.00	1.00	59.320	59.266	59.293	0.038	0.0014
7	1.00	–1.00	0.00	–1.00	19.640	19.510	19.575	0.092	0.0085
8	1.00	–1.00	–1.00	0.00	39.254	39.350	39.302	0.068	0.0046
9	–1.00	1.00	1.00	1.00	29.671	29.990	29.831	0.226	0.0511
10	–1.00	0.00	0.00	0.00	26.217	26.385	26.301	0.119	0.0142
11	1.00	1.00	1.00	0.00	19.952	19.990	19.971	0.027	0.0007
12	0.00	–1.00	1.00	0.00	39.340	39.970	39.655	0.445	0.1980
13	–1.00	–1.00	1.00	1.00	58.832	59.996	59.414	0.823	0.6773
14	0.00	0.00	–1.00	–1.00	12.829	12.796	12.813	0.023	0.0005
15	1.00	0.00	–1.00	1.00	39.531	39.208	39.370	0.228	0.0520
16	1.00	1.00	0.00	1.00	29.761	29.764	29.763	0.002	0.0000
17	1.00	–1.00	1.00	–1.00	19.910	19.980	19.945	0.049	0.0024
18	–1.00	1.00	–1.00	1.00	29.663	29.679	29.671	0.011	0.0001
19	0.00	1.00	0.00	–1.00	9.808	9.688	9.748	0.085	0.0072
20	1.00	0.00	1.00	–1.00	13.289	13.332	13.311	0.030	0.0009

Table 6
Results of the proposed WMSE model with the estimated process standard deviation

Case	w_1	w_2	x_1^*	x_2^*	x_3^*	x_4^*	Objective function	$\hat{\mu}(x)$	$\hat{\sigma}(x)$	$\lvert\hat{\mu}(x) - \mu_\tau\rvert$
1	0.0	1.0	1.0	0.9081	–0.1404	–1.0000	6.1164E-07	10.0135	0.0008	34.9865
2	0.1	0.9	1.0	–0.2441	0.1838	0.9918	0.0019	45.0043	0.0599	0.0043
3	0.2	0.8	1.0	–0.2662	–0.3502	0.9998	0.0026	45.0020	0.0750	0.0020
4	0.3	0.7	1.0	–0.2484	–0.0064	0.9987	0.0016	44.9999	0.0628	0.0001
5	0.4	0.6	1.0	–0.2294	0.3381	0.9964	0.0012	44.9993	0.0580	0.0007
6	0.5	0.5	1.0	–0.2113	0.6528	0.9927	0.0013	44.9961	0.0599	0.0039
7	0.6	0.4	1.0	–0.1974	0.8138	0.9948	0.0012	44.9980	0.0624	0.0020
8	0.7	0.3	1.0	–0.1851	0.9273	0.9984	0.0010	44.9995	0.0646	0.0005
9	0.8	0.2	1.0	–0.1779	0.9973	1.0000	7.3771E-04	44.9991	0.0664	0.0009
10	0.9	0.1	1.0	–0.1783	0.9962	0.9998	3.7069E-04	45.0008	0.0664	0.0008
11	1.0	0.0	1.0	–0.1784	0.9968	0.9997	2.0154E-06	45.0016	0.0664	0.0016

factor is not a significant factor based on the second-order model because the *p*-value is 0.760. Besides, each level affects ±0.070 mg/g for the removal process. Each case of the proposed optimization models resulted in +1.0000, and it means that the stirring speed is 1,000 rpm. Second, the adsorbent dosage is a significant factor based on the second-order model because the *p*-value is 0.000. Also, each level of the adsorbent dosage affects ±9.798 mg/g for the Pb(II) removal process. The center level of the adsorbent dosage approximately provided the optimum results for the removal process. It is also concluded that the YBS is an effective adsorbent to the Pb(II) removal process. Third, the pH level is not a significant factor based on the second-order model because the *p*-value is 0.191. Besides, each level of the pH level affects ±0.327 mg/g for the removal process. The optimum results of the pH level were usually obtained at high levels. Finally, the initial metal concentration is a significant factor based on the second-order model because the *p*-value is 0.000. Besides, it is the most important factor for the removal process. Each level of

Table 7
A comparison with other adsorbents

Adsorbent	Adsorption capacity (mg/g)	Studied by
Fly ash	20.55	Alinnor [34]
Natural zeolite tuff	78.00	Wang et al. [35]
Natural zeolite	66.00	Kragović et al. [36]
Calcite	132.95	Uçurum et al. [37]
White natural stone	43.66	Serencam et al. [38]
Yellow Bayburt stone	46.03	In this paper

the initial metal concentration affects ±14.777 mg/g for the Pb(II) removal process. For most cases in Table 6, the optimum results of the initial metal concentration were found at high levels.

The quadratic effects of adsorption factors were analyzed and the observations are made. The quadratic effect of the adsorbent dosage is a significant factor for the experiment. Each quadratic level of the adsorbent dosage affects ±2.763 mg/g for the removal process. On the other hand, other quadratic effects in the second-order model are not significant.

The interaction effects of adsorption factors were examined. The interaction effect of the adsorbent dosage and the initial metal concentration is significant in terms of the second-order model. Besides, each interaction level of the adsorbent dosage and the initial metal concentration affects ±5.047 mg/g for the removal process. On the contrary, other interaction effects in the second-order model are not significant. Therefore, the adsorbent dosage and the initial metal concentration are important to achieve more adsorption capacity for the removal process from the solution.

6. Concluding remarks

In this paper, a novel WMSE optimization model is proposed to obtain optimal conditions of adsorption factors for a lead removal process. Four adsorption factors, such as stirring speed (rpm), adsorbent dosage (g), pH level, and initial metal concentration (ppm), were investigated for the removal process from the solution. The five-phased methodology was demonstrated to find optimal conditions of adsorption factors. A *D*-optimal experimental design was selected to conduct the adsorption experiment. A full second-order model was used to analyze main, quadratic, and interaction effects for the adsorption experiment. A proposed WMSE optimization model is effective to obtain optimal conditions of adsorption factors while assigning different weights for each term in the objective function. The model validation and the verification study were also conducted. The optimum conditions are that stirring speed is 1,000 rpm, the adsorbent dosage is 0.69 g, pH is 4.7, and the initial metal concentration is 299.64 ppm. The mean values for the proposed model and the actual experiment are 44.9993 and 46.031 mg/g, respectively. It is also concluded that the adsorbent dosage and the initial metal concentration are significant adsorption factors to reach more adsorption capacity for the Pb(II) removal process from the solution. Besides, the yellow Bayburt stone is an effective and low-cost adsorbent for the adsorption experiment.

References

[1] Y. Bulut, Z. Baysal, Removal of Pb(II) from wastewater using wheat bran, J. Environ. Manage., 78 (2006) 107–113.
[2] J. Hamed, Y.B. Acar, R.J. Gale, Pb(II) removal from kaolinite by electrokinetics, J. Geotech. Eng-ASCE, 117 (1991) 241–271.
[3] G. Bereket, A.Z. Arog, M.Z. Özel, Removal of Pb(II), Cd(II), Cu(II), and Zn(II) from aqueous solutions by adsorption on bentonite, J. Colloid Interface Sci., 187 (1997) 338–343.
[4] B.E. Reed, R. Vaughan, L. Jiang, As(III), As (V), Hg, and Pb removal by Fe-oxide impregnated activated carbon, J. Environ. Eng., 126 (2000) 869–873.
[5] R. Naseem, S.S. Tahir, Removal of Pb(II) from aqueous/acidic solutions by using bentonite as an adsorbent, Water Res., 35 (2001) 3982–3986.
[6] V.C. Taty-Costodes, H. Fauduet, C. Porte, A. Delacroix, Removal of Cd(II) and Pb(II) ions, from aqueous solutions, by adsorption onto sawdust of *Pinus sylvestris*, J. Hazard. Mater., 105 (2003) 121–142.
[7] K.K. Wong, C.K. Lee, K.S. Low, M.J. Haron, Removal of Cu and Pb by tartaric acid modified rice husk from aqueous solutions, Chemosphere, 50 (2003) 23–28.
[8] B.M.W.P.K. Amarasinghe, R.A. Williams, Tea waste as a low cost adsorbent for the removal of Cu and Pb from wastewater, Chem. Eng. J., 132 (2007) 299–309.
[9] D. Xu, X. Tan, C. Chen, X. Wang, Removal of Pb(II) from aqueous solution by oxidized multiwalled carbon nanotubes, J. Hazard. Mater., 154 (2008) 407–416.
[10] K. Yetilmezsoy, S. Demirel, R.J. Vanderbei, Response surface modeling of Pb(II) removal from aqueous solution by *Pistacia vera* L.: Box–Behnken experimental design, J. Hazard. Mater., 171 (2009) 551–562.
[11] N.N. Nassar, Rapid removal and recovery of Pb(II) from wastewater by magnetic nanoadsorbents, J. Hazard. Mater., 184 (2010) 538–546.
[12] K. Al-Zboon, M.S. Al-Harahsheh, F.B. Hani, Fly ash-based geopolymer for Pb removal from aqueous solution, J. Hazard. Mater., 188 (2011) 414–421.
[13] G. Zhao, X. Ren, X. Gao, X. Tan, J. Li, C. Chen, Y. Huang, X. Wang, Removal of Pb(II) ions from aqueous solutions on few-layered graphene oxide nanosheets, Dalton Trans., 40 (2011) 10945–10952.
[14] C.J. Madadrang, H.Y. Kim, G. Gao, N. Wang, J. Zhu, H. Feng, M. Gorring, M.L. Kasner, S. Hou, Adsorption behavior of EDTA-graphene oxide for Pb(II) removal, ACS Appl. Mater. Interfaces, 4 (2012) 1186–1193.
[15] S.A. Kim, S. Kamala-Kannan, K.J. Lee, Y.J. Park, P.J. Shea, W.H. Lee, H.M. Kim, B.T. Oh, Removal of Pb(II) from aqueous solution by a zeolite–nanoscale zero-valent iron composite, Chem. Eng. J., 217 (2013) 54–60.
[16] Y. Liu, C. Yan, Z. Zhang, H. Wang, S. Zhou, W. Zhou, A comparative study on fly ash, geopolymer and faujasite block for Pb removal from aqueous solution, Fuel, 185 (2016) 181–189.
[17] Y. Ma, L. Lv, Y. Guo, Y. Fu, Q. Shao, T. Wu, S. Guo, K. Sun, X. Guo, E.K. Wujcik, Z. Guo, Porous lignin based poly (acrylic acid)/organo-montmorillonite nanocomposites: swelling behaviors and rapid removal of Pb(II) ions, Polymer, 128 (2017) 12–23.
[18] X. Liu, D. Lai, Y. Wang, Performance of Pb(II) removal by an activated carbon supported nanoscale zero-valent iron composite at ultralow iron content, J. Hazard. Mater., 361 (2019) 37–48.
[19] Z. Lin, X. Weng, G. Owens, Z. Chen, Simultaneous removal of Pb(II) and rifampicin from wastewater by iron nanoparticles synthesized by a tea extract, J. Cleaner Prod., 242 (2020) 118476.
[20] G.G. Vining, R.H. Myers, Combining Taguchi and response surface philosophies: a dual response approach, J. Qual. Technol., 22 (1990) 38–45.

[21] B.R. Cho, Optimization Issues in Quality Engineering, Ph.D. Dissertation, School of Industrial Engineering, University of Oklahoma, Norman, OK, 1994.
[22] D.K. Lin, W. Tu, Dual response surface optimization, J. Qual. Technol., 27 (1995) 34–39.
[23] B.R. Cho, M.D. Philips, K.C. Kapur, Quality Improvement by RSM Modeling for Robust Design, The 5th Industrial Engineering Research Conference, Minneapolis, 1996, pp. 650–655.
[24] O. Köksoy, N. Doganaksoy, Joint optimization of mean and standard deviation using response surface methods, J. Qual. Technol., 35 (2003) 239–252.
[25] B.R. Cho, Y.J. Kim, D.L. Kimbler, M.D. Phillips, An integrated joint optimization procedure for robust and tolerance design, Int. J. Prod. Res., 38 (2000) 2309–2325.
[26] R. Ding, D.K. Lin, D. Wei, Dual-response surface optimization: a weighted MSE approach, Qual. Eng., 16 (2004) 377–385.
[27] S. Shin, F. Samanlioglu, B.R. Cho, M.M. Wiecek, Computing trade-offs in robust design: Perspectives of the mean squared error, Comput. Ind. Eng., 60 (2011) 248–255.
[28] O. Köksoy, Multiresponse robust design: mean square error (MSE) criterion, Appl. Math. Comput., 175 (2006) 1716–1729.
[29] H. Park, S.H. Park H.B. Kong, I. Lee, Weighted sum MSE minimization under per-BS power constraint for network MIMO systems, IEEE Commun. Lett., 16 (2012) 360–363.
[30] A. Ozdemir, B.R. Cho, A nonlinear integer programming approach to solving the robust parameter design optimization problem, Qual. Reliab. Eng. Int., 32 (2016) 2859–2870.
[31] A. Ozdemir, B.R. Cho, Response surface-based robust parameter design optimization with both qualitative and quantitative variables, Eng. Optimiz., 49 (2017) 1796–1812.
[32] A. Ozdemir, B.R. Cho, Response surface optimization for a nonlinearly constrained irregular experimental design space, Eng. Optim., 51 (2019) 2030–2048.
[33] H. Şahin, Investigation of Usability of Tuffs Called as Bayburt Stone as a Mineral Admixture in Cement Production, Master Thesis, Department of Civil Engineering, Graduate School of Natural and Applied Sciences, Bayburt University, Bayburt, Turkey, 2018.
[34] I.J. Alinnor, Adsorption of heavy metal ions from aqueous solution by fly ash, Fuel, 86 (2007) 853–857.
[35] S. Wang, T. Terdkiatburana, M.O, Tadé, Adsorption of Cu(II), Pb(II) and humic acid on natural zeolite tuff in single and binary systems, Sep. Purif. Technol., 62 (2008) 64–70.
[36] M. Kragović, A. Daković, Ž. Sekulić, M. Trgo, M. Ugrina, J. Perić, D.G. Gatta, Removal of lead from aqueous solutions by using the natural and Fe(III)-modified zeolite, Appl. Surf. Sci., 258 (2012) 3667–3673.
[37] M. Uçurum, A. Özdemir, Ç. Teke, H. Serencam, M. İpek, Optimization of adsorption parameters for ultra-fine calcite using a Box-Behnken experimental design, Open Chem., 16 (2018) 992–1000.
[38] H. Serencam, A. Özdemir, Ç. Teke, M. Uçurum, Modeling design parameters with Taguchi experimental method for obtaining operating conditions for Cu(II) removal through adsorption process, Desal. Water Treat., 167 (2019) 269–276.